



Contents lists available at ScienceDirect

Journal of King Saud University – Science

journal homepage: www.sciencedirect.com

Assessment of green and chemically synthesized copper oxide nanoparticles against hepatocellular carcinoma

M. Fakhar-e-Alam^a, Zahra Shafiq^a, Arslan Mahmood^a, M. Atif^b, Hafeez Anwar^c, Atif Hanif^d, Nafeesah Yaqub^b, W.A. Farooq^b, Amanullah Fatehmulla^b, Shafiq Ahmad^e, Abd Elatty E. Abd Elgawad^e, K.S. Alimgeer^f, Tuan Nguyen Gia^{g,*}, Hijaz Ahmed^{h,i,*}

^a Department of Physics, Government College University Faisalabad, Faisalabad 38000, Pakistan

^b Department of Physics and Astronomy, College of Science, King Saud University, Riyadh 11451, Saudi Arabia

^c Department of Physics, University of Agriculture Faisalabad, 38000 Faisalabad, Pakistan

^d Botany and Microbiology Department, College of Science, King Saud University, Riyadh 11451, Saudi Arabia

^e Industrial Engineering Department, College of Engineering, King Saud University, P.O. Box 800, Riyadh 11421, Saudi Arabia

^f Department of Electrical and Computer Engineering, COMSATS University, Islamabad, Islamabad Campus, Pakistan

^g Department of Computing, University of Turku, 20500 Turku, Finland

^h Department of Basic Sciences, University of Engineering and Technology, Peshawar 25000, Pakistan

ⁱ Section of Mathematics, International Telematic University Uninettuno, Corso Vittorio Emanuele II, 39, 00186 Roma, Italy

ARTICLE INFO

Article history:

Received 26 May 2021

Revised 5 October 2021

Accepted 19 October 2021

Available online 26 October 2021

Keywords:

Chemical synthesis

Green synthesis

Anti-carcinoma activity

Liver carcinoma

Mathematical modeling

ABSTRACT

Copper oxide nanoparticle (CuO-NPs) attracts the attentions of human beings due to unique physico-chemical and biological properties. The chemical and green synthesis approaches were used to synthesis of CuO-NPs and plant leaves extract *Azadirachta indica* (*A. indica*) was preferred in green synthesis approach. The XRD analysis was used to analyze the monoclinic crystal structure and calculate the average crystallite size in the range of 15 ~ 16 nm. While, the information about different rotational and vibrational modes attached on the spectrum of CuO-NPs was identified by FTIR. After that the UV-VIS analysis provided the information about the absorbance spectrums in the range of 235 and 220 nm. The MTT assay was performed to investigate liver carcinoma (HepG2 cells) interaction and absorbance of CuO-NPs towards mentioned cell lines were recorded and loss in HepG2 cells viability. In an overall assessment, anticancer response of comparative study of CuO-NPs towards liver carcinoma treatment contributes significantly after successful demonstration of essential steps of suggested experimental study. Finally, comparative study of experimental and mathematical modeling of anticancer activity towards normal and liver cancer cell lines were conducted and investigated.

© 2021 The Author(s). Published by Elsevier B.V. on behalf of King Saud University. This is an open access article under the CC BY-NC-ND license (<http://creativecommons.org/licenses/by-nc-nd/4.0/>).

1. Introduction

Cancer is an alarming health problem and is becoming the main cause of mortality worldwide. The increasing rate of cancer cases might be due to unhealthy diet, consumption of alcohol and

tobacco (Golshah et al., 2019; Vinardell and Mitjans, 2015). Considering the current situation early recognition and appropriate experimental strategy are the basic need of present situation. Many oncologists and researchers work in the field of medical science are trying to resolve the serious health issues. Nowadays, the researchers are played the central role to overcome cancer diagnostic and treatment problems (Shaheen et al., 2017). Continuous efforts have been made to deliver adequate health care benefits at the least possible cost to improve survivability (Sivaraj et al., 2014; Vinardell and Mitjans, 2018; Verma and Kumar, 2019; Rehman et al., 2018a; Ur Rehman et al., 2019).

Previously, available therapies are not suitable for the treatment of carcinoma due to multiple side effects. It was very difficult to differentiate the normal and carcinoma cells. Likewise, the therapies are also damage the healthy cells. These problems were

* Corresponding authors at: Department of Computing, University of Turku, 20500 Turku, Finland (T.N. Gia).

E-mail addresses: tuan.nguyengia@hotmail.com (T.N. Gia), hijaz555@gmail.com (H. Ahmed).

Peer review under responsibility of King Saud University.



Production and hosting by Elsevier

solved to use the transition metals base NPs for the treatment of carcinoma by using different therapies (Sankar et al., 2014; Ramaswamy et al., 2016; Yugandhar et al., 2017; Munir et al., 2019; Naz et al., 2020a,b). Moreover, CuO-NPs are attract the attention of researcher due to incredible properties such as biocompatible, low toxicity, small particle size, high surface area, stability, biodegradability, reasonable bandgap (1.73 eV), small crystallite size and decrease the recombination of charge carriers of CuO-NPs (Ghidan et al., 2016; Kalaiarasi et al., 2018). Presently, CuO-NPs are considered significant due to their excellent catalytic, electrical, textile, intrinsic anticancer activities, gas sensors, biomedicines and environmental remediation (Dey et al., 2019). However, CuO-NPs toxicity influence towards bacterial, algae, fish, rats, human cell lines are remarkable (Naz et al., 2020a,b; Sivaraj et al., 2014; Vasantharaj et al., 2019). It helps to destruction of DNA and slows down the growth rate of cancer bearing cells by releasing copper ions from CuO-NPs induce apoptosis of tumor cells. The CuO-NPs are synthesized by using different methods to attain cost efficiency and reduce time consumption. Among various methods such as sol-gel, microwave, sonochemical, various toxic reducing agents, co-precipitation and extract of plants as reducing agent have been used to synthesize the CuO-NPs (Awwad et al., 2015; Wu et al., 2002; El-Trass et al., 2012; Tadjarodi and Roshani, 2014).

The previous study was provided the information about the chemically synthesis approach of CuO-NPs to improve the toxicity level for living things. The chemical used during synthesis process irritate skin, nose and eyes. Moreover, the excess used of CuO-NPs cause respiratory system, gastro intestinal tract and skin related diseases. In case of green synthesis approach reduces the toxicity level of CuO-NPs and medicinal green plant was preferred due to cost effective, biocompatible and eco-friendly (Padil and Černík, 2013; Devi and Singh, 2014; Yugandhar et al., 2017). This study focused to synthesis of CuO-NPs via chemical and green synthesis approaches. *Azadirachta indica* (*A. indica*) is the common name of Neem plant that is used in green synthesis approach of CuO-NPs. *A. indica* is a medicinal plant that used to cure the multiple diseases. The multiple characterization techniques such as XRD, FTIR, and UV-VIS were used for material analysis and MTT assay for anti-carcinoma activity. Finally, the prepared CuO-NPs towards mentioned cells were recorded and loss in HepG2 cells viability was assessed by MTT assay.

2. Experimental procedures

2.1. Green synthesis approach

The green synthesis approach was used for the synthesis of CuO-NPs. The fresh leaves *Azadirachta indica* (Neem) were washed twice and cut into small pieces. After that 20 g leaves were dissolved in 100 mL de-ionized water and boiled at 60 °C for 20 min. Likewise, prepared solution was filtered by using filter paper and 2 g of $C_4H_8CuO_5$ mixed in 20 mL solution boiled at 80 °C to get the green color mixture. Moreover, the product was dried in an oven and then put into furnace at 400 °C for 2 h. Finally, black color precipitate was grinded in mortar and pestle. The schematic diagram of CuO-NPs for treatment of hepatocellular carcinoma is shown in Fig. 1.

2.2. Chemical synthesis approach

The chemical approach was used for the synthesis of CuO-NPs in which copper chloride (0.06 M) was dissolved in 200 mL de-ionized water and continuous stirred on magnetic stirrer for

30 min. The NaOH (0.15 M) solution was prepared to attain the pH upto 11 of copper chloride solution. The prepared solution was continuously stirred on magnetic stirrer for 3 h to get black color homogeneous mixture. After that, prepared solution was filter by using filter paper with the help of de-ionized water. Finally, the black color product was dried in oven at 80 °C for 2 h. The prepared precipitate of black color powder was grinded in mortar and pestle.

2.3. Material characterizations techniques

The following are the characterization techniques were used to characterize the CuO-NPs powder. The XRD (Cu-K α radiation 1.5406 Å (D8 Advance, Bruker, X'Pert3 MRD XL) was used to study the crystalline nature of required nanomaterial. To identify the different rotational and vibrational modes were attached on the spectrum of CuO-NPs with the help of FTIR (Spectrum 2, Perkin Elmer). The absorbance bands of CuO-NPs were recorded using UV-VIS (Lambda 25, Perkin Elmer) (Munir et al., 2021).

2.4. Bioassay

2.4.1. HepG2 cell culturing

HepG2 (liver cancer cells) cell lines 1×10^4 cells/well and normal human liver cells THLE-2 derived from liver (human) epithelial cells were cultured in 96 well plates. The 25 cm plastic tissue culture flasks and 96 wells plates (Nunc Wiesbaden Germany) individually in DMEM with (10%) fetal bovine serum and Hanks salts. After that 2 mM/L glutamine with some non-essential amino acids were incubated for 24 h. The atmosphere was provided to culture cell lines at 37 °C and it was subcultured three times a week. The 65–75% cell cultured indicate that the confluence was harvested by using trypsin 0.25% (Alam et al., 2012a,b; Alam et al., 2021; Govarathanan et al., 2016).

2.4.2. Cell labeling with CuO-NPs

The stock solution of CuO-NPs via chemical approach as well as green synthesis approach were prepared having compound polarity solution of 100 mg/L by dispersing/considering working solution of CuO-NPs (0, 10, 20, 40, 60, 80 and 100 μ g/mL) incorporated into HepG2 cells cultured. Experimental arrangement of 96 wells plate and first ten columns of 96 well plate having confluence of 85% of hepG2 cells confluence were allocated for localized CuO-NPs test and rest of two columns of 96 wells plate were reserved for control/reference HepG2 cells.

2.4.3. MTT assay

The HepG2 cancer cells lines were tested by employing MTT assay (Alam et al., 2015). This assay was used to study the living cells in which active mitochondria. It was responsible to convert the tetrazolium compound into formazan product (insoluble purple colour). Moreover, CuO-NPs were labeled HepG2 cells lines and fixed in MTT for 3 hrs at 37 °C. After that three times washed cell lines and drying at room temperature under the presence of dry air and its color were dissolved in DMSO. Only 15 min of shaking, the plates were assessed using Multiscan MCC/340 microplate reader at filters (540 and 490 nm) respectively. Finally, the photodynamic treatment and cellular viability of cancer cells lines were estimated by applying MTT assay. The percentage feasible cell in each test was calculated by using standard method (Wu et al., 2002; Rehana et al., 2017, Alam et al., 2020).

$$\% \text{ Viability} = \frac{\text{Mean Absorbance of ALA treated cells}}{\text{Means Absorbance of control cells}} \times 100$$

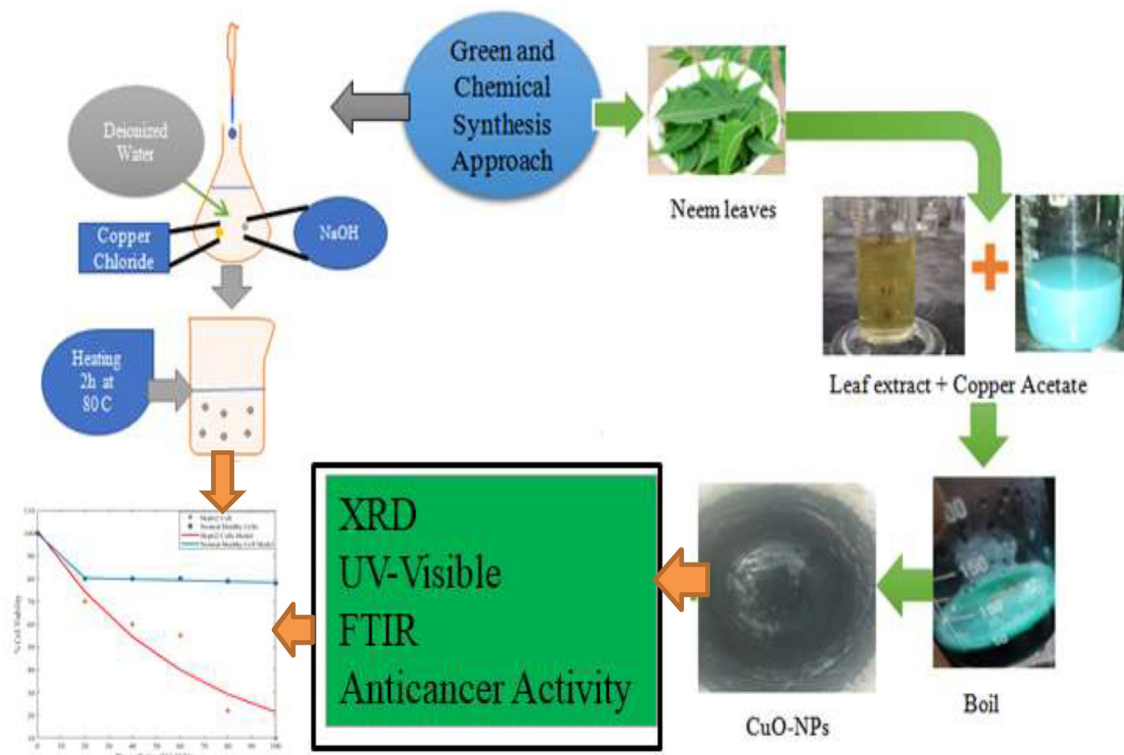


Fig. 1. Schematic diagram of CuO-NPs for treatment of hepatocellular carcinoma.

3. Results and discussion

3.1. XRD measurement

The XRD analysis was used to identify the crystal structure and calculate the crystallite size of CuO-NPs obtained through green and chemical synthesis approach. XRD pattern of CuO-NPs as shown in Fig. 2(a) green synthesis and Fig. 2(b) Chemical synthesis approach represented the monoclinic phase and matched well with (JCPDS-80-1916) card (Awwad, et al., 2015). In both cases, the same pattern was observed and no extra peak appeared in case of green synthesis method. The green synthesis peaks indicate slight fluctuation as compare to chemical approach. The different

diffracted peaks indicate the 2θ values at 32.3, 35.7, 38.4, 48.9, 53.1, 58.5 corresponding to following miller indices such as $(\bar{1} 1 0)$, (002), (111), $(\bar{2} 0 2)$, (020) and (202) (Awwad et al., 2015; Zhao et al., 2013). Furthermore, the crystallite size of these NPs was calculated by using the scherrer equation. The average crystallite size (CuO-NPs) for chemical and green synthesis approach in between (15 ~ 16 nm) as expressed in Table 1.

3.2. FTIR measurement

The FTIR analysis was used identify the different rotational and vibrational modes attached on the spectrum of CuO-NPs. Fig. 3 exhibited FTIR spectrum of CuO-NPs (a) green synthesis approach

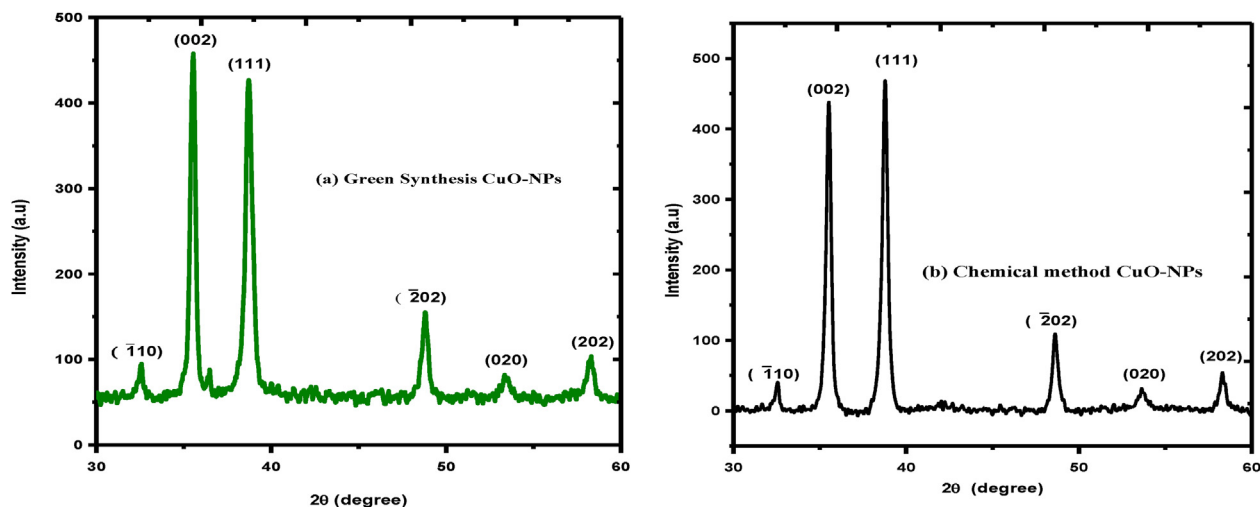


Fig. 2. XRD spectrum of CuO-NPs (a) green synthesis (b) chemical approach.

Table 1
Crystallite size of green and chemical synthesis CuO-NPs.

CuO-NPs	Peak (002)	Peak (111)	Average size (nm)
Green synthesis	18	14	16
Chemical approach	17	13	15

(b) chemical synthesis approach. Fig. 3(a) indicates the peak of CuO-NPs is shifted, when the reaction between plants leaves extract and copper nitrate take place. The FTIR spectrum of CuO-NPs represented that the broader absorption band at 3742 cm^{-1} - corresponds to the hydroxyl (OH) functional group. The few other absorption peaks were observed at different wavenumber 2360 cm^{-1} IR band at 1537 cm^{-1} can be assigned to alkenes group (C=C). Moreover, the peaks at 1535 cm^{-1} indicate stretching vibration of C-O group due to the presence of alcohols (C-O) at 1537 , while smaller peaks at 780 and 768 cm^{-1} and 465 cm^{-1} were assigned vibration of C-H group. Fig. 3(b) chemical approach range from 450 to 4500 cm^{-1} . At $3500\text{--}3700\text{ cm}^{-1}$ indicate the OH stretching vibrational mode, while the band $1647\text{--}1689$ represents 1st amide and $1500\text{--}1530$ shows 2nd amide region. Finally, the bands $500\text{--}600\text{ cm}^{-1}$ indicated that metal oxide (CuO-NPs) due to the vibration in monoclinic phase (Sharma et al., 2015).

3.3. UV-visible spectroscopy measurement

Here, UV-VIS analysis was used to study the absorbance spectra of CuO-NPs Fig. 4(a) green synthesis Fig. 4(b) chemical synthesis approach. Fig. 4 shows that the absorbance band at 235 nm for chemical synthesis and 220 nm for green synthesis approach CuO-NPs respectively. Furthermore, UV-VIS spectroscopy of CuO-NPs shows blue shift as compare to CuO bulk close agreement with previous publishes data (Zain et al., 2007).

3.4. Antioxidant and tumoricidal activities of green synthesis as well as chemically synthesized CuO-NPs (experimental as well as mathematical modulated comparison)

In this section the cell viability loss (%) due to biosynthetic procedure of CuO-NPs were demonstrated which depicts that beyond a certain concentration of CuO-NPs ($20\text{ }\mu\text{g/mL}$) the cell viability loss in HepG2 cell were significant but superficial effects of green synthesized CuO-NPs towards health liver cells were counted/recorded which identify the satisfactory and great development in field of biomedical science. In addition, experimental and mathematical modeling results reflect very good agreement in overall cell viability loss trend seen in Fig. 5 compare with our previous

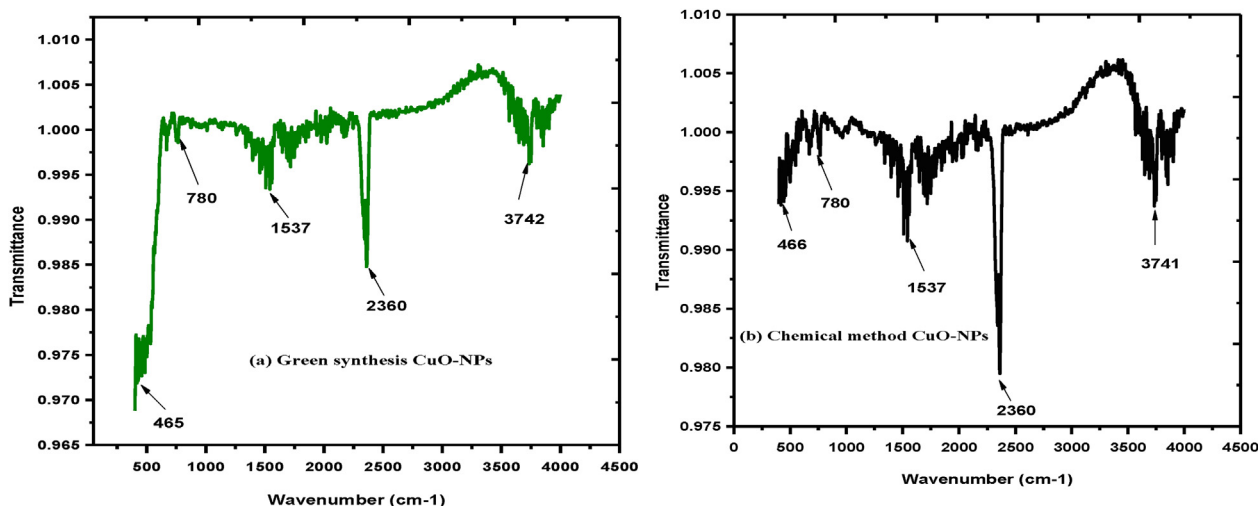


Fig. 3. FTIR spectrum of CuO-NPs (a) green synthesis approach (b) chemical synthesis approach.

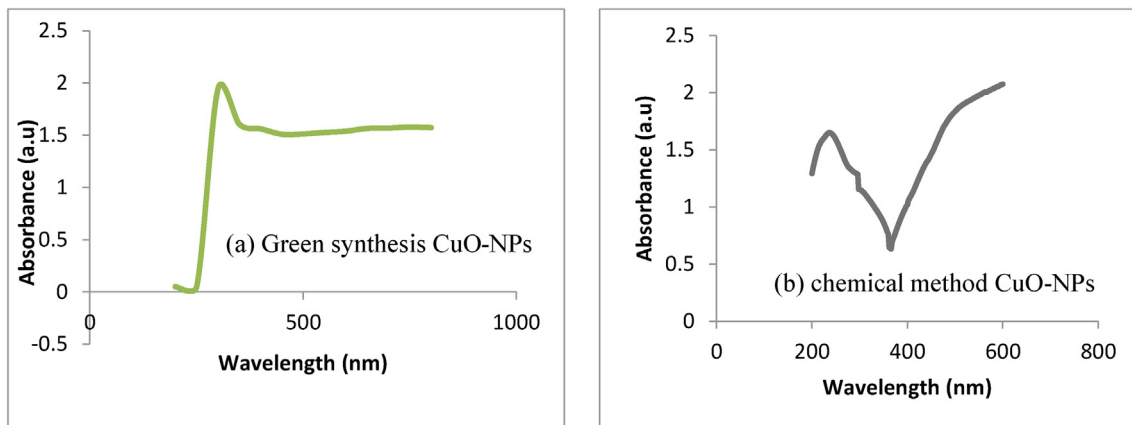


Fig. 4. UV-VIS spectra of CuO-NPs (a) green synthesis approach (b) chemical synthesis approach.

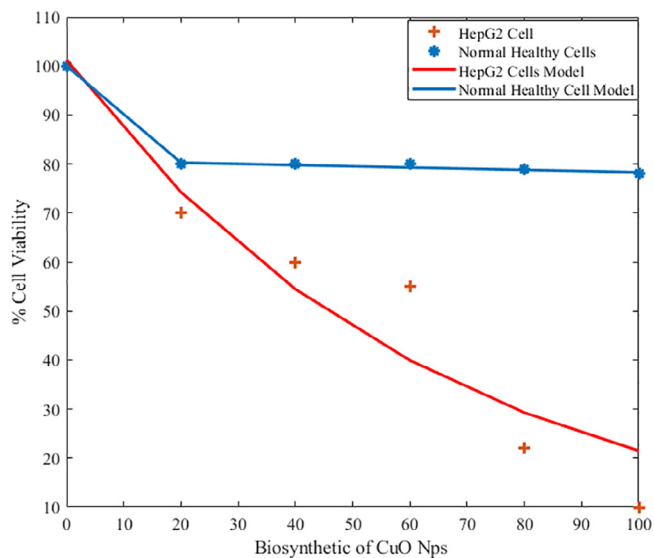


Fig. 5. Comparative study of tumoricidal effect (loss in cell Viability %) of biosynthetic of CuO-NPs (microgram/mL) in healthy liver and HepG2 cells (modeling and Experimental Data).

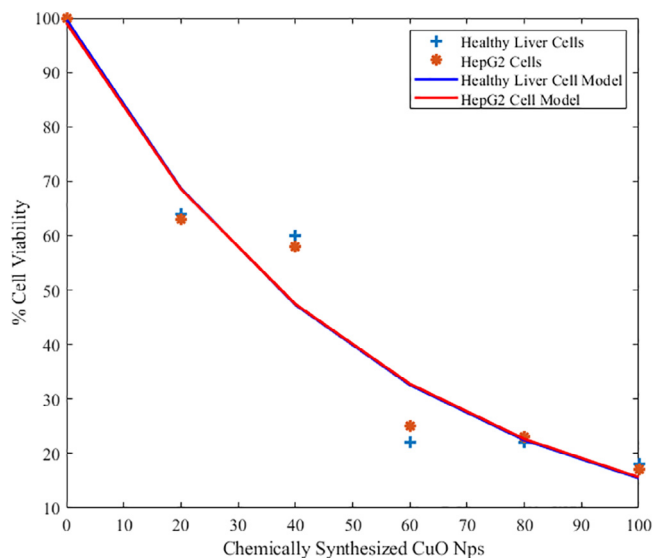


Fig. 6. Comparative study of tumoricidal effect (loss in cell Viability %) of chemically synthesized CuO-NPs (microgram/mL) in healthy liver and HepG2 cells (modeling and experimental data).

published data (Alam et al., 2015). Similar pattern of results was recorded, which of course depicts the non-invasiveness of photodynamic therapy.

The chemically synthesized CuO-NPs, very toxic effects towards normal healthy liver were investigated along with HepG2 cells (liver cancer cells). As compared to green synthesis procedure of CuO-NPs grown material, chemical synthesized materials are not feasible for PDT as cell viability loss of experimental and modeling data were shown in Fig. 3.5.

The cytotoxic effect of green and chemical synthesis approach of CuO-NPs was tested against normal healthy liver and HepG2 cell lines. Moreover, the Fig. 6 indicated that % cell viability by applying CuO-NPs of both mathematical modeling and experimental analysis. The analysis represented that CuO-NPs provided the significant toxicity effect toward liver carcinoma. The low density lipoproteins (LDL) in liver cancer cells provided the toxicity and the LDL have excellent ability to attract the antioxidant agents. The CuO-NPs occupied the different type of antioxidant due to this ability; it was used for the treatment of liver carcinoma. Few other types of chemical reaction take place inside the cells by applying the nanoparticles and these nanoparticle create the oxidative stress due to loss of membrane was used to kill the carcinoma cells. The significance of this experiment is that first time reported the comparison of chemical and green synthesis approach of CuO-NPs. The cell viability loss 85% of liver carcinoma call and approximately 15% loss of healthy cells were calculated. But in case of green synthesis approach only target the carcinoma cells and these nanoparticles have no any side effect on the healthy cells. Similar pattern of study were conducted in the previous published data (Alam et al., 2012a,b; AlSalhi et al., 2020).

$$Model = a \times e^b + c \times e^d \tag{1}$$

Eq. (1) shows the proposed mathematical model. This type of model is known as bi-exponential model due to the presence of two weighted summation of exponential functions. This model is used to find fitness of experimental data collected from 4 different experiments. These experiments were conducted using biosynthetic CuO-NPs for healthy and HepG2 cells. Similarly, another experimental setup is established for chemically synthesized CuO-NPs for healthy and HepG2 cells. The data is experimentally collected from above said procedure and used to extract different parameters appeared in Eq. (1). The parameters are extracted using method of least square errors and listed in Table 2. Figure of merits for the goodness of fit are also evaluated such as SSE, R-square, Adjusted R- Square (A R-square) and RMSE and listed in the Table 2. A Mat lab was used to written the extract these model parameters along with goodness of fit (Jain et al., 2007). Moreover, ROS confirms the DNA damage via ROS detection assay and try pan blue staining assay. Results depicted that CuO nanoparticle responsible for DNA damage which leads to oxidative stress lesions causes' cell viability loss.

Table 2

Represented the parameters through the method of least square errors used in Eq. (1) along with figure of merits for the goodness of fit.

Biosynthetic		A	B	C	D
	HepG2	101	-0.0155	0	0
	Healthy	19.24	-0.9901	10.76	-0.0003083
		SSE	R-Square	A R-square	RMSE
	HepG2	462.2	0.9138	0.8922	10.75
	Healthy	0.2728	0.9992	0.9981	0.3693
Chemically Synthesized		A	B	C	D
	HepG2	99.64	-0.01862	0	0
	Healthy	-192.3	-0.02001	291.3	-0.01945
		SSE	R-Square	A R-square	RMSE
	HepG2	301.8	0.9436	0.9296	8.686
	Healthy	206.2	0.9599	0.8998	10.15

It can be observed that in biosynthetic of CuO-NPs, the healthy cells have stable behaviour for % cell viability and did not dropped below 80% for increasing biosynthetic of CuO-NPs (Islas et al., 2020). Likewise; HepG2 cells have dropped % cell viability below 15%. This particular behaviour shows that the normal healthy cell will remain unaffected while the HepG2 cells are affected drastically. On the other side, chemically synthesized CuO-NPs have shown the drastic drop of % cell viability for both normal health cells and for HepG2 cells. Mathematical functions in terms of bi-exponential model are presented for any future comparison.

4. Conclusion

The chemical and green synthesis approach was used to synthesize the CuO-NPs. In case of green synthesis approach the plant leaves extract of *Azadirachta indica* (*A. indica*) was used to prepare the CuO-NPs. The XRD depicted monoclinic phase and the crystallite size in the range 15 to 16 nm. After that the FTIR spectrum was used to identify the presence of different rotational and vibrational modes attached on the spectra of CuO-NPs. The UV-VIS analysis represented the absorbance peaks at 220 and 235 nm. In vitro MTT assay towards HepG2 was carried out for the determination of anti-carcinoma activity comprises of chemical and green synthesized of CuO-NPs. By using green synthesis approach, the development of CuO-NPs shows significant toxicity towards liver carcinoma and it proved bio-safe towards healthy liver tissue island when assessed MTT assay. But opposite relation of chemically grown CuO-NPs were recorded. We conclude that CuO-NPs synthesized using *Azadirachta indica* (*A. indica*) leaves extract may be implemented as chemotherapeutic agents for anticancer activity which significantly play a vital role for cancer treatment purpose in near future.

Declaration of Competing Interest

The authors declare that they have no known competing financial interests or personal relationships that could have appeared to influence the work reported in this paper.

Acknowledgement

Researchers Supporting Project number (RSP-2021/397), King Saud University, Riyadh, Saudi Arabia.

References

Alam, M.F., Aseer, M., Rana, M.S., Aziz, M.H., Atif, M., Yaqub, N., Farooq, W.A., 2020. Spectroscopic features of PHOTOGEN[®] in human Rhabdomyosarcoma (RD) cellular model. *J. King Saud Univ.-Sci.* 32 (7), 3131–3137.

Alsalhi, M.S., Aziz, M.H., Atif, M., Fatima, M., Shaheen, F., Devanesan, S., Aslam Farooq, W., 2020. Synthesis of NiO nanoparticles and their evaluation for photodynamic therapy against HeLa cancer cells. *J. King Saud Univ.-Sci.* 32 (2), 1395–1402.

Awwad, A.M., Albiss, B.A., Salem, N.M., 2015. Antibacterial activity of synthesized copper oxide nanoparticles using *Malva sylvestris* leaf extract. *SMU Med. J.* 2 (1), 91–101.

Devi, H.S., Singh, T.D., 2014. Synthesis of copper oxide nanoparticles by a novel method and its application in the degradation of methyl orange. *Adv. Electron. Electr. Eng.* 4 (1), 83–88.

Dey, A., Manna, S., Chattopadhyay, S., Mondal, D., Chattopadhyay, D., Raj, A., Das, S., Bag, B.G., Roy, S., 2019. *Azadirachta indica* leaves mediated green synthesized copper oxide nanoparticles induce apoptosis through activation of TNF- α and caspases signaling pathway against cancer cells. *J. Saudi Chem. Soc.* 23 (2), 222–238.

El-Trass, A., ElShamy, H., El-Mehasseb, I., El-Kemary, M., 2012. CuO nanoparticles: synthesis, characterization, optical properties and interaction with amino acids. *Appl. Surf. Sci.* 258 (7), 2997–3001.

Fakhar-e-Alam, M., Ali, S.M.U., Ibutoto, Z.H., Kimpleang, K., Atif, M., Kashif, M., Loong, F.K., Hashim, U., Willander, M., 2012a. Sensitivity of A-549 human lung cancer

cells to nanoporous zinc oxide conjugated with Photofrin. *Lasers Med. Sci.* 27 (3), 607–614.

Fakhar-e-Alam, M., Kishwar, S., Abbas, N., Atif, M., NURC, O., Willander, M., Farooq, W.A., 2015. Anticancer effects of nanometallic oxides and their ligands with photosensitizers in osteosarcoma cells. *J. Optoelectron. Adv. Mater.* 17, 1808–1815.

Fakhar-e-Alam, M., Kishwar, S., Siddique, M., Atif, M., Nur, O., Willander, M., 2012b. The photodynamic effect of ZnO nanorods and their ligands with different photosensitizers. *Rev. Nanosci. Nanotechnol.* 1 (1), 40–51.

Ghidan, A.Y., Al-Antary, T.M., Awwad, A.M., 2016. Green synthesis of copper oxide nanoparticles using *Punica granatum* peels extract: Effect on green peach Aphid. *Environ. Nanotechnol. Monit. Manage.* 6, 95–98.

Golshah, A., Taran, M., Safaei, M., Mozaffari, H.R., Imani, M.M., Sharifi, R., Moradpoor, H., Upadhyay, P., 2019. Applying the Taguchi method to the optimization of anticancer activity of bacterial alginate-CuO bionanocomposite. *Open Access Macedonian J. Med. Sci.* 7 (1), 1–5.

Govarthanan, M., Cho, M., Park, J. H., Jang, J. S., Yi, Y. J., Kamala-Kannan, S., & Oh, B. T. (2016). Cottonseed oilcake extract mediated green synthesis of silver nanoparticles and its antibacterial and cytotoxic activity. *J. Nanomater.* 2016.

Jain, P.K., Huang, X., El-Sayed, I.H., El-Sayed, M.A., 2007. Review of some interesting surface plasmon resonance-enhanced properties of noble metal nanoparticles and their applications to biosystems. *Plasmonics* 2 (3), 107–118.

Kalaiarasi, A., Sankar, R., Anusha, C., Saravanan, K., Aarthi, K., Karthi, S., Ravikumar, V., 2018. Copper oxide nanoparticles induce anticancer activity in A549 lung cancer cells by inhibition of histone deacetylase. *Biotechnol. Lett.* 40 (2), 249–256.

Munir, T., Mahmood, A., Fakhar-e-Alam, M., Imran, M., Sohail, A., Amin, N., Mahmood, K., 2019. Treatment of breast cancer with capped magnetic-NPs induced hyperthermia therapy. *J. Mol. Struct.* 1196, 88–95.

Munir, T., Mahmood, A., Imran, M., Sohail, A., Fakhar-e-Alam, M., Sharif, M., Latif, S., 2021. Quantitative analysis of glucose by using (PVP and MA) capped silver nanoparticles for biosensing applications. *Physica B* 602, 412564.

Naz, S., Tabassum, S., Freitas Fernandes, N., Mujahid, M., Zia, M., Carcache de Blanco, E.J., 2020a. Anticancer and antibacterial potential of *Rhus punjabensis* and CuO nanoparticles. *Nat. Prod. Res.* 34 (5), 720–725.

Naz, S., Gul, A., Zia, M., 2020b. Toxicity of copper oxide nanoparticles: a review study. *IET Nanobiotechnol.* 14 (1), 1–13.

Padil, V.V.T., Černík, M., 2013. Green synthesis of copper oxide nanoparticles using gum karaya as a biotemplate and their antibacterial application. *Int. J. Nanomed.* 8, 889.

Ramaswamy, S.V.P., Narendhran, S., Sivaraj, R., 2016. Potentiating effect of ecofriendly synthesis of copper oxide nanoparticles using brown alga: antimicrobial and anticancer activities. *Bull. Mater. Sci.* 39 (2), 361–364.

Rehana, D., Mahendiran, D., Kumar, R.S., Rahiman, A.K., 2017. Evaluation of antioxidant and anticancer activity of copper oxide nanoparticles synthesized using medicinally important plant extracts. *Biomed. Pharmacother.* 89, 1067–1077.

Ur Rehman, K.M., Liu, X., Riaz, M., Yang, Y., Feng, S., Khan, M.W., Khan, M., Raslan, E. H., 2019. Fabrication and characterization of Zinc Telluride (ZnTe) thin films grown on glass substrates. *Physica B* 560, 204–207.

Rehman, K.M.U., Liu, X., Feng, S., Khan, M.W., Wazir, Z., Zongyang, Z., Li, H., 2018a. Influence of temperature on Sr 0.35 La 0.40 Ca. 25 Fe 11.6 Co 0.4 O 19 hexagonal ferrites against structural, morphological and magnetic properties prepared by conventional ceramic reaction methodology. *J. Supercond. Novel Magn.* 31 (3), 925–932.

Islas, J.F., Acosta, E., G-Buentello, Z., Delgado-Gallegos, J.L., Moreno-Treviño, María G., Escalante, B., Moreno-Cuevas, J.E., 2020. An overview of Neem (*Azadirachta indica*) and its potential impact on health. *J. Funct. Foods* 74, 104171. <https://doi.org/10.1016/j.jff.2020.104171>.

Sankar, R., Maheswari, R., Karthik, S., Shivashangari, K.S., Ravikumar, V., 2014. Anticancer activity of *Ficus religiosa* engineered copper oxide nanoparticles. *Mater. Sci. Eng., C* 44, 234–239.

Shaheen, F., Hammad Aziz, M., Fakhar-e-Alam, M., Atif, M., Fatima, M., Ahmad, R., Ahmed, M., 2017. An in vitro study of the photodynamic effectiveness of GO-ag nanocomposites against human breast cancer cells. *Nanomaterials* 7 (11), 401.

Sharma, J.K., Akhtar, M.S., Ameen, S., Srivastava, P., Singh, G., 2015. Green synthesis of CuO nanoparticles with leaf extract of *Calotropis gigantea* and its dye-sensitized solar cells applications. *J. Alloy. Compd.* 632, 321–325.

Sivaraj, R., Rahman, P.K.S.M., Rajiv, P., Narendhran, S., Venkatesh, R., 2014. Biosynthesis and characterization of *Acalypha indica* mediated copper oxide nanoparticles and evaluation of its antimicrobial and anticancer activity. *Spectrochim. Acta Part A Mol. Biomol. Spectrosc.* 129, 255–258.

Tadjarodi, A., Roshani, R., 2014. A green synthesis of copper oxide nanoparticles by mechanochemical method. *Curr. Chem. Lett.* 3 (4), 215–220.

Vasantharaj, S., Sathiyavimal, S., Saravanan, M., Senthilkumar, P., Gnanasekaran, K., Shanmugavel, M., Manikandan, E., Pugazhendhi, A., 2019. Synthesis of ecofriendly copper oxide nanoparticles for fabrication over textile fabrics: characterization of antibacterial activity and dye degradation potential. *J. Photochem. Photobiol., B* 191, 143–149.

Verma, N., Kumar, N., 2019. Synthesis and biomedical applications of copper oxide nanoparticles: an expanding horizon. *ACS Biomater. Sci. Eng.* 5 (3), 1170–1188.

Vinardell, M.P., Mitjans, M., 2015. Antitumor activities of metal oxide nanoparticles. *Nanomaterials* 5 (2), 1004–1021.

Vinardell, M.P., Mitjans, M., 2018. Metal/metal oxide nanoparticles for cancer therapy. *Nanooncology*, 341–364.

Wu, H.Q., Wei, X.W., Shao, M.W., Gu, J.S., Qu, M.Z., 2002. Synthesis of copper oxide nanoparticles using carbon nanotubes as templates. *Chem. Phys. Lett.* 364 (1-2), 152–156.

Yugandhar, P., Vasavi, T., Devi, P.U.M., Savithramma, N., 2017. Bioinspired green synthesis of copper oxide nanoparticles from *Syzygium alternifolium* (Wt.)

Walp: characterization and evaluation of its synergistic antimicrobial and anticancer activity. *Applied Nanoscience* 7 (7), 417–427.

Zhao, J., Wang, Z., Dai, Y., Xing, B., 2013. Mitigation of CuO nanoparticle-induced bacterial membrane damage by dissolved organic matter. *Water Res.* 47 (12), 4169–4178.